Preparation of ceramic coatings on titanium formed by micro-arc oxidation method for biomedical application

M. M. DICU[*], M. ABRUDEANU, S. MOGA, D. NEGREA, V. ANDREI[a], C. DUCU
[*]University of Pitesti, Research Center for Advanced Materials, Targu din Vale, No 1, 110040, Pitesti, Romania
[a]DIMat-R, Renault Technologies Romania, Uzinei, No 1-3, 115400, Mioveni, Arges, Romania

This paper presents a method to grow nano-structured TiO_2 by micro-arc oxidation (MAO) on titanium surfaces. During the oxidation treatment, the titanium sample was immersed in electrolytic solution containing calcium acetate monohydrate $(CH_3COO)_2Ca \cdot H_2O$) and sodium phosphate monobasic dihydrate ($NaH_2PO_4 \cdot 2H_2O$). During the process of the simulated body fluid (SBF) immersion (3 day in SBF and 3 day in 5SBF), the Ca and P of the MAO coating dissolves into the SBF, increasing the supersaturation degree near the surface of the MAO coating, which could promote the formation and growth of apatite. The morphologies on the sample surfaces were observed by scanning electron microscopy (SEM). The oxide film composition was semi-quantitatively analyzed with an electron probe microanalyzer (EDX). X-Ray Diffraction (XRD) analysis was used to determine the phase composition of the coatings prepared by MAO at different treatment time. Fourier Transform Infrared Spectroscopy (FT-IR) was used to analyze the phase and structure of the MAO coatings after SBF immersion.The coatings were rough and porous, without apparent interface to the titanium substrates. All the oxidized coatings contained Ca and P as well as Ti and O, and the porous coatings were made up of anatase, rutile and hydroxyapatite.

1. Introduction

Micro-arc oxidation (MAO) is a recently developed technique which can produce a porous, relatively rough, and firmly adherent titanium oxide film on titanium surface [1,2].

MAO has been employed for modifying the surface of titanium and its alloys intended to use as biomaterials, or for improving the mechanical properties of these materials. By applying a positive voltage to a Ti substrate immersed in an electrolyte, when the applied voltage is increased to a certain point, a micro-arc occurs and a TiO_2 layer on the surface is formed. The MAO coatings are beneficial to cell attachment and bone growth and shows better apatite forming ability [3].

Titanium, characterized by good strength, low density, high melting point, is a biocompatible material and its biocompatibility can be improved by surface treatments. Titanium and its thin naturally formed oxide films are known to be bio-inert, therefore, unlike other bioactive materials such as bioglasses and calcium phosphate ceramics, allows the osteointegration process at the interface titanium-tissue, instead of bone-bonding.

Titanium and its alloys are widely and successfully used in medicine as implant materials. The longevity of implants (dental implants and orthopaedic prostheses) depends on the integration of the implant with the surrounding bone. A very important role in the osteointegration is played by the ability of the surface to spontaneously form hydroxyapatite (HA) in the body fluid. Titanium has many advantageous properties but its ability to form HA on its surface is not as good as that of some ceramics. To improve the osteointegration, the implants are often coated with hydroxyapatite layers. Recently, great interest has been placed on the surface modification by MAO [4–6]. This technique yields rough and porous ceramic layers, whose composition depends on the chemical composition of the electrolyte solution employed and on the substrate material.

Ishizawa and Ogino [7–9] were first to make use of the MAO method for producing hydroxyapatite layers on titanium. They produced the layers using a two-step process: in the first step they enriched the titanium oxide layer with calcium and phosphorus by the MAO method and then transformed the Ca- and P enriched oxide layers into hydroxyapatite using a hydrothermal treatment.

The growth of coatings under MAO conditions enables modification of oxide properties compared with conventional anodizing below the sparking voltage, such as thickness, chemical composition, crystal structure, porosity, topography and roughness, [10], which have been shown to influence the bone response [11,12]. Sul et al. demonstrated that strong reinforcement of bone tissue reactions occurs with anatase-containing coatings >600 nm thick, with a porous surface morphology [11]. The structures of anodic films and MAO coatings on titanium

are greatly affected by species incorporated into the coating from the electrolyte, with crystallinity being suppressed in coatings-containing silicon, phosphorus and calcium species [13–18].

The object of this study was to explore porous titanium inner-pore wall modification by MAO, with the emphasis on the structural characteristics of the anodized films (including morphology, phase component, element composition). In vitro bioactivity of the oxidized specimens was investigated by immersing them into SBF or 5 SBF and examining the extent of apatite formation on their surfaces.

2. Experimental details

Titanium specimens $14 \times 16 \times 3$ mm^3 in size were cut from a sheet of titanium (commercially pure titanium - grade 2) and used as substrate. The chemical composition of the raw material is: Fe 0.105 %; C 0.011 %; O 0.175 %; N 0.006 %; H 0.0005 % and Ti.

Prior to MAO treatment, the titanium plates were polished using #200 – #1000 SiC sandpaper gradually, degreased and successively cleaned in an ultrasonic bath with ethyl alcohol and distilled water.

The MAO equipment was design and manufactured at the University of Pitesti within the Research Center for Advanced Materials. The experimental set-up consists of: an insulated stainless steel electrolyte cell with a stirrer and a pulsed bipolar DC power supply. The titanium plate was used as anode, while a stainless steel cell was used as cathode. The electrolyte in the electrolyte cell was an aqueous solution containing 0.13 mol/l calcium acetate monohydrate $((CH_3\text{-}COO)_2Ca \cdot H_2O)$ and 0.06 mol/l sodium biphosphate dihydrate $(NaH_2PO_4 \cdot 2H_2O)$ in distilled water.

MAO was carried out at an applied voltage of 400 V for 15, 20, 30 and 45 min. During the oxidation, the temperature of electrolyte was less than 50°C. After the MAO treatment, the samples were washed with distilled water and dried at room temperature.

The oxidizes sample was immersed in a SBF solution with the following composition: NaCl 7.9344 g/L, NaHCO$_3$ 0.350 g/L, KCl 0.222 g/L, K$_2$HPO$_4$ 0.174 g/L, MgCl$_2$.6H$_2$O 0.303 g/L, CaCl$_2$.6H$_2$O 0.545 g/L, Na$_2$SO$_4$.10H$_2$O 0.161 g/L, for 3 day and then in a solution 5 SBF (a solution with Ca^{2+} concentration 5 times higher) for another 3 days [19].

The morphology of treated surfaces was observed on a Scanning Electron Microscope (SEM, Low-vaccum Inspect S – FEI Company). The elemental composition was studied with energy dispersive X-ray spectrometer (EDX, Genesis-XM2) incorporated into the scanning electron microscope. EDX was performed at an acceleration voltage of 20 kV.

The X-ray diffraction (XRD) measurements were performed on a Rigaku Ultima IV system (CuK$_\alpha$ radiation) with Parallel Beam optics. The divergence angle of emitted beam from the multilayer mirror is approximately 0.05^0. This kind of optics is suitable for analysis because of increased beam intensity and significant reduction of instrumental aberrations.

For the qualitative phase analysis the X-ray diffraction patterns were acquired in Bragg-Brentano geometry, in the 2θ range 20^0-73^0, step width 0.05^0 and 5s as counting time. Also, grazing incidence geometry was used to obtain surface structural information by measuring the MAO coatings under small incidence angle. The angle of the incident beam was fixed at 1° and the X-ray diffraction measurements were recorded in the same 2θ range.

The Fourier Transform Infrared (FTIR) spectra were processed with a Jasco 620 spectrophotometer for detecting the element groups of the samples.

3. Results and discussion

3.1. Morphology of the micro-arc oxidation film (SEM)

Fig. 1 (a-d) shows SEM micrographs of the surfaces of titanium substrates treated with MAO in the Ca- and P-containing solution. The porous and rough surface with micropores is formed due to a high temperature in discharge channels during the MAO process. The pores were well separated and homogeneously distribute over the surface. The pore diameter varies from 2 to 9 μm. The holes in the surface were channels of micro-arc discharge in electrolyte.

Usually, porous and rough surface morphology are preferable choices for biomaterials. Pores in the film not only favors the anchorage of implants to bone, but also acts as nucleation sites for bone tissue, thereby a saturation of the precipitated apatite granular in pores could quickly be reached [20]. In the same tine, the porous structure with nano-sized pores was shown to be far more effective in inducing apatite formation [21,22].
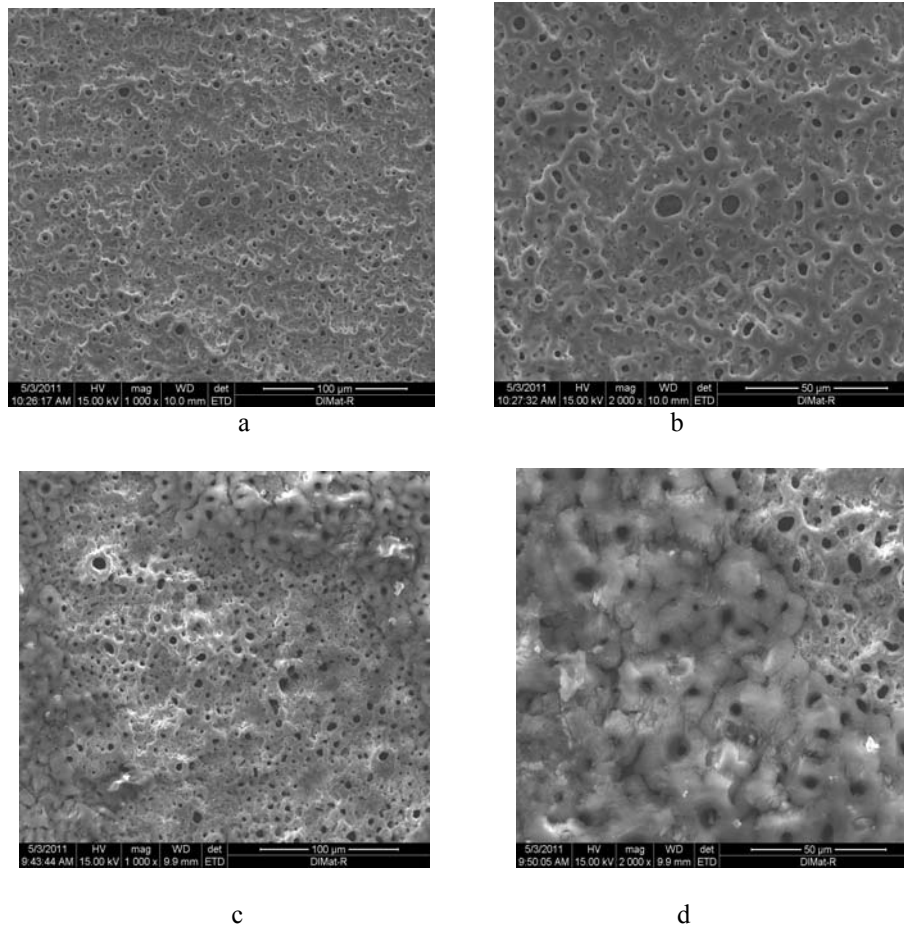
Fig. 1. SEM surface morphologies at different magnification of titanium samples treated with MAO :
(a-b) 400 V for 30 min and (c-d) 400 V for 45 min

3.2. Elemental composition of the micro-arc oxidation film (EDX)

SEM micrograph presented in Fig. 2a. indicates that the surface of the 45 min treated MAO sample is not chemically homogeneous, with regions being richer in Ca and P. It can easily be noticed fine precipitates gathered in grains (region 2).

The extent of Ca and P incorporation in the oxidized layer was determined by EDX as it is shown in Fig. 2 (b-c). As the oxidation time increased, the content of O hardly changed and the content of Ti decreased, but the content of Ca and P increased evidently.
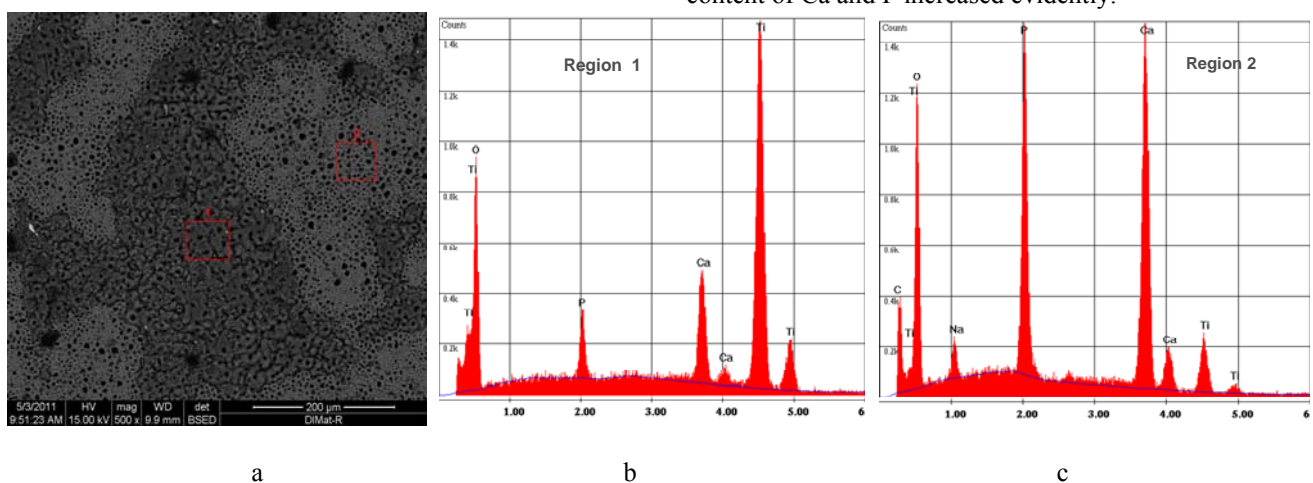

Fig. 2. (a) Morphology, (b-c) EDX spectrums of the micro-arc oxidation film prepared at 400 V for 45 min

For the first area, the calculated [Ca] / [P] ratio from EDX measurements was 1.86 (standard ratio for hydroxyapatite is 1.67). It is believed that the enrichment of Ca and P at the surface can improve bioactivity of the titanium implant [23].

Examinations of the ability of titanium surface to nucleate hydroxyapatite have shown that the nucleation depends on the amount of the hydroxyl groups that are present on the titanium surface [24]. Hanawa et al. [23] reported that the quantity of hydroxyl groups on the surface of Ca-implanted titanium is greater than that on nonimplanted titanium. The formation mechanism of calcium phosphates on the titanium surface consists of two stages: first the phosphate ions from the solution bind to the hydroxyl groups through a hydrogen bond, and then the phosphate ions attract the Ca ions from the solution [24]. The greater the amount of hydroxyl groups on the surface, the greater the number of adsorbed phosphate ions, and in turn, the greater the number of Ca ions attracted from the solution. As a result, the number of precipitates of calcium phosphate on the surface increases. Ca present in the surface coating gradually dissolves and passes into the surrounding solution thereby increasing the pH and the concentration of Ca ions beyond the titanium surface, which produces effects that promote the nucleation of calcium phosphate.

3.3. Microstructure of the micro-arc treated specimen (XRD)

The recorded symmetrical θ/2θ X-ray diffraction patterns for the obtained MAO coatings are shown in Fig. 3. The intensity is plotted in arbitrary units. As we can see in the figure, the coatings are highly crystalline and mainly composed of a mixture of anatase and rutile phases.
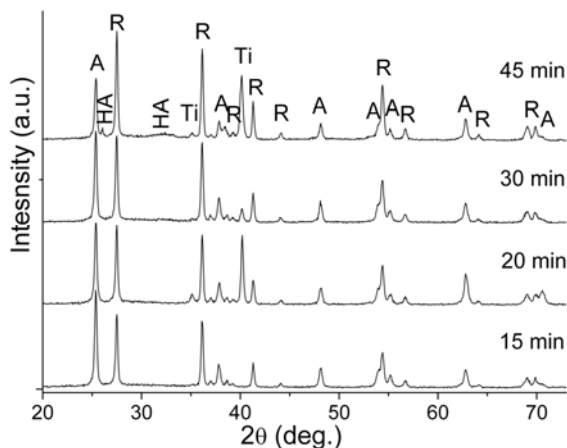

Fig. 3. XRD patterns of the MAO coatings at different treatment time: A-anatase, R-Rutile, Ti – Titanium alpha; HA – hydroxyapatite

We can observe that the structure of the layers evolved with the oxidation time. When the treatment was 15 min, no titanium alpha reflections related to the substrate were found in the XRD pattern, suggesting that

this sample had the thicker coating. The intensities of the rutile Bragg reflections increased with the treatment time.

Although EDX analysis revealed the presence of Ca and P species on the surface of all the samples, the polycrystalline HA appeared in the XRD pattern only at 45 min treatment, the profiles of the diffraction lines being broad and diffuse due to poor crystallization of the HA.

From the XRD patterns recorded at α=1⁰ incidence angle (see Fig. 4) we can observe that the predominant TiO_2 phase in the surface is the rutile. Also, the reflections related to HA were more obvious.
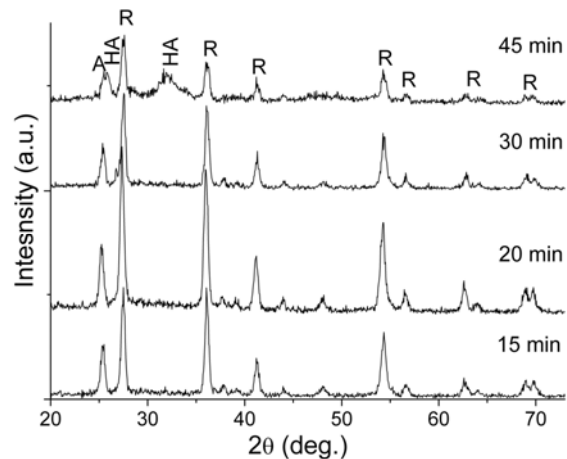

Fig. 4. GIXRD patterns at α=1⁰ of the MAO coatings at different treatment time.

Along with the Bragg reflections corresponding to the rutile phase, several low-intensity anatase reflections could also be identified.

The predominance of rutile in the coating surface confirms that the local temperature of the plasma at the surface of the sample was very high, due to high voltages used here [25]. For bulk samples, the transformation temperature of metastable anatase to rutile is over 900°C, and rutile is a more thermally stable phase [26].

3.4. The apatite layer formation of the MAO coatings in SBF

After 3 day immersion in SBF and then in a solution 5 SBF for other 3 days, Ca and P containing precipitates were formed on the surface of the oxide films resulting in a reduction of Ca and P concentrations in the SBF. After immersing for a pre-determined period of time, the samples were removed from the SBF, then washed with distilled water and then dried.

The results obtained for the samples oxidized and soaked in SBF indicate that the SBF solution (with following composition: NaCl 7.9344 g/L, $NaHCO_3$ 0.350 g/L, KCl 0.222 g/L, K_2HPO_4 0.174 g/L, $MgCl_2.6H_2O$ 0.303 g/L, $CaCl_2.6H_2O$ 0.545 g/L, $Na_2SO_4.10H_2O$ 0.161 g/L) does not change significantly the chemical composition of the layer. The phase changes of the oxidized films during immersion in the SBF were

investigated by XRD and no noticeable changes were observed after 6 days of immersion.

Fig. 5 show the surface morphology for the oxidized sample at 400 V and 45 minutes after six days immersion in SBF. This surface present a rough and porous characteristic of the micro-arc oxidized layer.
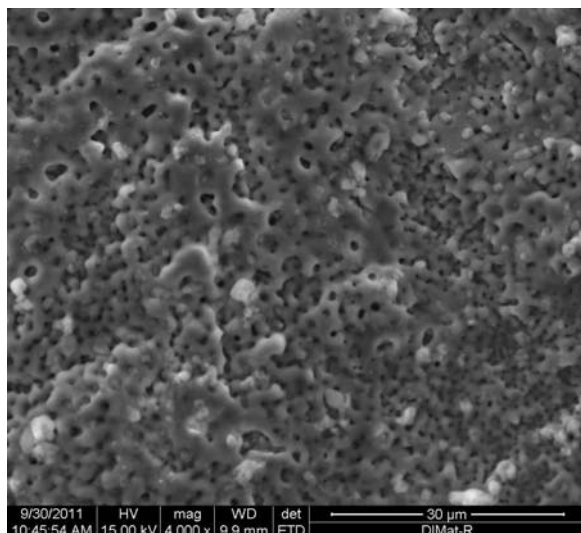

Fig. 5. Morphology of the micro-arc oxidation film (400 V, 45 min) soaked in the 5SBF for 3 days.

The MAO coating oxidized at 400 V and immersed in SBF six days, induces hydroxyapatite formation. The process in confirmed by FT-IR results (Fig. 6) through the presence of PO_4^{-3} and OH^- along with a CO_3^{2-} absorption band.
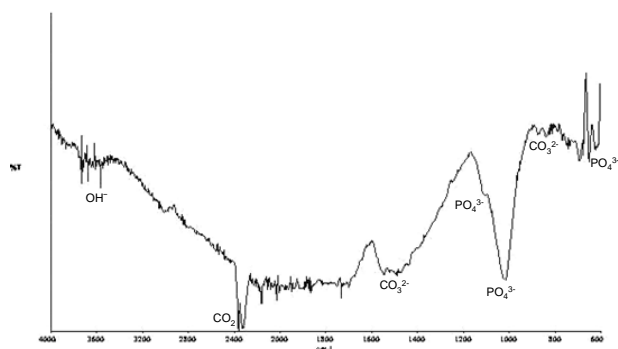

Fig. 6. FT-IR spectrums of the sample oxidized at 400 V, 45 min and soaked in the SBF for 6 days.

The band around 1095 cm^{-1}/1018 cm^{-1} and 610 cm^{-1} are assigned to ν 3 P-O band and ν 4 P-O band in PO_4^{3-}, respectively. The CO_3^{2-} absorption band is also detected by the characteristic stretching mode of the CO_3^{2-} group at 1460 cm^{-1} and the characteristic OH^- bands of HA at 3560 cm^{-1} are not clearly visible, indicating that carbonate incorporated to apatite and formed carbonate-apatite [27]. The CO_3^{2-} would be generated from the decomposition of

$(CH_3COO)^-$ or the absorption of atmospheric CO_2 at ambient temperature [28].

SBF is a metastable calcium phosphate solution supersaturated with respect to apatite. However, it was reported that a barrier for the homogeneous nucleation of apatite is too high and a chemical stimulus is required to induce the heterogeneous nucleation of apatite from the SBF [29].

4. Conclusions

The TiO_2 coatings were successfully obtained on commercially titanium (grade 2) by MAO using an electrolytic solution containing calcium acetate monohydrate $(CH_3COO)_2Ca \cdot H_2O$ and sodium phosphate monobasic dihydrate $(NaH_2PO_4 \cdot 2H_2O)$.

The morphology and chemical composition of the coatings obtained by MAO process depend on the treatment time. The oxide layers formed were rough, porous, and enriched with Ca and P.

The XRD pattern obtained for the oxidized samples shows that the oxide layer is principally composed of TiO_2 anatase and rutile. The phase ratio is variable. The content of rutile increased while the anatase content decreases. With the increasing of the oxidation time, it can be observed the apparition of hydroxyapatite phase.

The Infrared (FT-IR) data confirmed HA formation through the existence of hydroxyl, carbonate and phosphate bands. The accumulated grains of apatite are mainly composed of hydroxyapatite (HA) and carbonate–apatite.

References

[1] Y. Han, K. Xu, J. Biomed., Mater. Res.,
    71A, 608 (2004).
[2] W.H. Song, Y.K. Jun, Y. Han, S.H. Hong, Biomat.,
    25, 3341 (2004).
[3] D.Y. Kim, M. Kim, H.E. Kim, Y.H. Koh, H.W. Kim,
    J.H. Jang , Acta Biomater, **5**, 2196 (2009).
[4] G.P. Wirtz, S.D. Brown, W.M. Kriven, Mater. Manuf.
    Processes, **6**, 87 (1991).
[5] A.L. Yerokhin, X. Nie, A. Leyland, A. Matthews,
    S.J. Dowey, Surf. Coat. Technol. **122**, 73 (1999).
[6] F.C. Walsh, C.T.J. Low, R.J.K. Wood, K.T. Stevens,
    J. Archer, A.R. Poeton, A. Ryder, Trans. Inst. Met.
    Finish. **87**, 122 (2009).
[7] H. Ishizawa, M. Ogino, J. Biomed. Mater. Res.,
    29, 65 (1995).
[8] H. Ishizawa, M. Ogino, J. Biomed. Mater. Res.,
    29, 1071 (1995).

[9] H. Ishizawa, M. Fujino, M. Ogino, J. Biomed. Mater. Res., **29**, 1459 (1995).

[10] Y.-T. Sul, C.B. Johansson, S. Petronis, A. Krozer, Y. Jeong, A. Wennerberg, Biomat., **23**, 491 (2002).

[11] Y.-T. Sul, Biomat., **24**, 3893 (2003).

[12] Y.-T. Sul, C. Johansson, E. Byon, T. Albrektsson, Biomat., **26**, 6720 (2005).

[13] E. Matykina, M. Montuori, J. Gough, F. Monfort, A. Berkani, P. Skeldon, Trans. Inst. Met. Finish **84**, 125 (2006).

[14] H. Habazaki, K. Shimizu, S. Nagata, P. Skeldon, G.E. Thompson, G.C. Wood, Corros. Sci. **44**, 1047 (2002).

[15] H. Habazaki, K. Shimizu, S. Nagata, P. Skeldon, G.E. Thompson, G.C. Wood, J. Electrochem. Soc., **149** B, 70 (2002).

[16] H. Habazaki, M. Uozumi, H. Konno, K. Shimizu, P. Skeldon, G.E. Thompson, Corros. Sci., **45**, 2063 (2003).

[17] E. Matykina, F. Monfort, A. Berkani, P. Skeldon, G.E. Thompson, P. Chapon, Phil. Mag. **86**, 49 (2006).

[18] E. Matykina, F. Monfort, A. Berkani, P. Skeldon, G.E. Thompson, J. Gough, J. Electrochem. Soc. **154** C, 279 (2007).

[19] F. Li, Q.L. Feng, F.Z. Cui, H.D. Li, H. Scubert, Surface and Coat. Tech., **154**, 88 (2002).

[20] L.L. Hench, J. Am. Ceram. Soc., **81**, 1705 (1998).

[21] P.J. Li, C. Ohtsuki, T. Kokubo, K. Groot, J. Biomed. Mater. Res., **28**, 7 (1994).

[22] H.M. Kim, F. Miyaji, T. Kokubo, S. Nishiguchi, J. Biomed. Mater. Res., **45**, 100 (1999).

[23] H. Hanawa, M. Kon, H. Doi, H. Ukai, K. Murakami, H. Hamanaka, J. Mater. Med., **9**, 89 (1998).

[24] T. Kokubo, Mater. Sci. Eng., **25**C, 97 (2005).

[25] A.L. Yerokhin, A. Leyland, A. Matthews, Surf. Coat. Technol., **200**, 172 (2002).

[26] L.L. Hench, J. Wilson, An Introduction to Bioceramics, (World Scientific Publishing, Singapore), p. 181 (1993).

[27] B.S. Ng, I. Annergren, A.M. Soutar, K.A. Khor, A.EW Jarfors, Biomaterials, **26**, 1087 (2005).

[28] Y. Han, J.F. Sun, X. Huang, Electrochem. Commun., **10**, 510 (2008).

[29] P. Li, I. Kangasniemi, K. de Groot, T. Kokubo, J. Am. Ceram. Soc. **77**, 1307 (1994).

*Corresponding author: ela_magda@yahoo.com